International Journal of Mass Spectrometry 277 (2008) 142–150

Contents lists available at ScienceDirect

International Journal of Mass Spectrometry

journal homepage: www.elsevier.com/locate/ijms

Absolute dissociative electron attachment cross-sections of chloro- and bromo-ethylenes

Yury V. Vasil'ev[a,b,*], Valery G. Voinov[a,c], Douglas F. Barofsky[a], Max L. Deinzer[a,d,*]

[a] Department of Chemistry, 153 Gilbert Hall, Oregon State University, Corvallis, OR 97331, USA
[b] Department of Physics, Bashkir State Agricultural University, Ufa, Russia
[c] Pacific Institute of Bioorganic Chemistry, Vladivostok, Russia
[d] Department of Biochemistry and Biophysics, Oregon State University, Corvallis, OR 97331, USA

ARTICLE INFO

Article history:
Received 11 April 2008
Received in revised form 1 July 2008
Accepted 15 July 2008
Available online 25 July 2008

Dedicated to Professor Eugen Illenberger on the occasion of his 65th birthday.

Keywords:
Resonant electron capture mass spectrometry
Negative ions
Absolute electron attachment cross-sections
Halo-ethylenes

ABSTRACT

Resonant electron capture by C_2Cl_4, C_2HCl_3, *cis*-, *trans*- and geminal-$C_2H_2Cl_2$, C_2HBr_3, *cis*- and *trans*-$C_2H_2Br_2$ and C_2H_3Br has been studied. A new method for the measurements of absolute electron attachment cross-sections based on the interface of a gas-chromatography and a reflectron-time-of-flight-mass spectrometer has been developed and the method was applied for these compounds.

1. Introduction

Eugen Illenberger and his group contributed tremendously [1–3] to our knowledge of resonant electron attachment/capture by different halogenated compounds, including haloethylenes [4,5]. Low-energy gas-phase reactions between electrons and haloethylenes resulting in the formation of negative ions (NIs) [6–23] or the associated transitions into dipole-allowed or dipole-forbidden neutral excited states [24,25] have been a subject of very intense investigations during the past several decades. Thermochemical characteristics of NIs formed in these reactions also have been reported [26–28]. The great interest in these compounds is associated with their atmospheric and environmental significance [29,30] as well as with their participation in electron transfer reactions that occur with metal containing molecules catalyzed by biologically relevant compounds, like vitamin B_{12} [31,32]. Rate constants for reductive dechlorination, has been found to decrease with decreasing halogen content in these reactions. To better understand the kind of physical or chemical processes involved and link these processes with the chemical reactivity of the compounds, it is important to gain knowledge of the rate constants or the cross-sections of elementary electron-capturing gas-phase reactions. The absolute rate constants or the cross-sections of the electron attachment reactions have been studied at length in the case of chloro-ethylenes [6–12]. However, there is no general agreement in the data obtained by different methods nor is there any consistency in the data from similar experimental measurements. Accordingly, a general method that yields reliable and reproducible results is needed.

Based on recently described [33,34] gas chromatograph/resonant electron capture-time-of-flight-mass spectrometry (GC–REC-TOF-MS), the present paper deals with the development of a new method for the determination of absolute negative ion formation cross-sections. Due to the very short acquisition time for three-dimensional REC mass spectra, this instrument is capable of recording the spectra of effluents from a capillary GC column in real time. Thus several mixtures of compounds have been separated by GC and their REC spectra recorded [34]. This technological advance provided an opportunity to further develop

* Corresponding authors.
E-mail addresses: Y.Vasilev@orst.edu (Y.V. Vasil'ev), Max.Deinzer@oregonstate.edu (M.L. Deinzer).

1387-3806/$ – see front matter © 2008 Elsevier B.V. All rights reserved.
doi:10.1016/j.ijms.2008.07.008

a method to obtain absolute electron attachment cross-sections by introduction of the calibrant and analyte in known molar ratios through the GC column. The main concern in this approach is to insure that the particular GC column is equally suitable for the analytes and calibration compounds. In these investigations the absolute electron attachment cross-sections have been determined for chloro-ethylenes as well as for bromo-ethylenes, which to our knowledge, have not been reported yet.

2. Computational methods

The starting geometry of the haloethylenes was based on results from semi-empirical calculations at the PM3 level of theory. The data were further used for calculations of the electronic and geometric structures of neutral molecules and their molecular and fragment NIs using Hartree-Fock SCF (6-31G*) theory that have been proved to reliably predict energies of shape resonances when using scaling procedures [35,36]. Analytical frequency analyses confirmed that the HF/6-31G(d)-optimized geometries have no imaginary frequencies. The results from these calculations also have been used for Rice–Ramsperger–Kassel–Marcus (RRKM) estimations of electron autodetachment rate constants in the case of $C_2Cl_4^-$ and $C_2HCl_3^-$ NIs.

3. Experimental

The instrument used in the present work has been described in detail elsewhere [33,34] and therefore only some specific peculiarities of the experimental conditions will be briefly described here. A trochoidal electron monochromator (TEM) capable of producing an electron current of several nano-amperes with an energy spread of 40–200 meV (full width at half maximum, FWHM) was used. The electron energy was ramped from 0 to 12 eV. The compounds under study and the calibrant were dissolved in either pentane or hexane, which themselves are practically transparent with respect to electron attachment. Depending on the GC retention time of the compounds studied, hexane and pentane were alternated to prevent any interference on the time scale with the compounds studied and avoid the pressure effects in the ion source. Two calibrant compounds, CCl_4 and $CHCl_3$, whose electron attachment cross-section are well known [37,38], were used simultaneously. The values of Cl^- production, 9.63×10^{-16} cm^2 at 0.27 eV ($CHCl_3$) and 4.5×10^{-16} cm^2 at 0.8 eV (CCl_4) reported most recently [38] were used as references. Net cross-sections were obtained by averaging over 6–7 runs and by comparing these average values with both calibrant compounds via the following equation:

$$\sigma_x = \frac{\sigma_{cal} I_x n_{cal} V_{cal} M_x}{I_{cal} n_x V_x M_{cal}}, \quad (1)$$

where subscripts x and cal are respectively the compound under study and calibrant; σ, is the cross-section; I, the measured ion signal; n, the density number; V, injected volume and M, the molecular mass.

The present measurements gave slightly lower ratios for the calibrant Cl^- cross-sections (~1.7 instead of ~2 as in [37,38]) and therefore accuracy of our measurements is within ~10–15% in addition to the reported accuracy [38] that is ~10%. In the present experiments, mixtures of the haloethylenes under study (volume ratio from 1 to 100) and pentane/hexane–CCl_4–$CHCl_3$ (ratios 1000, 1, 1) were injected (0.5 μL) into the GC (DB-624 column; He flow was 3 mL/min; the temperature programmed from 30 to 150 °C) at 4 °C/min. CCl_4, $CHCl_3$ together with low pressure (<10^{-7} Torr) SF_6-gas introduced through a separate gas port, were used for calibration of cross-sections, electron energy and mass scales. Research grade haloethylenes were purchased from Sigma–Aldrich and were used without further purification.

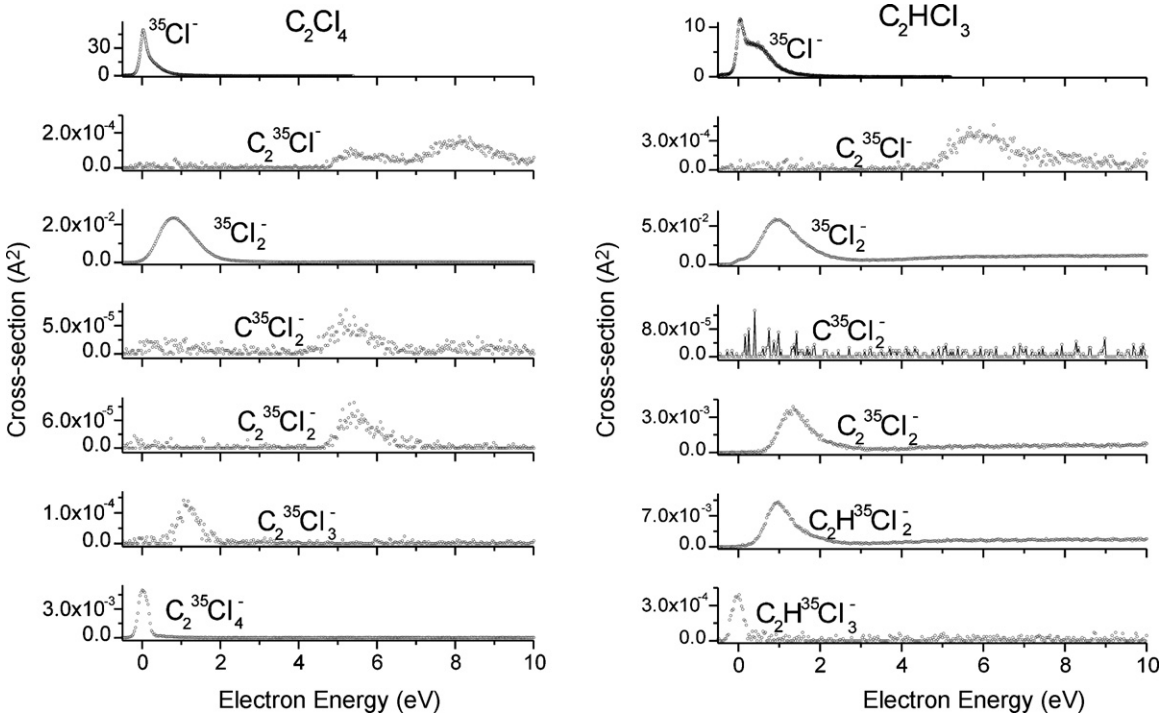

Fig. 1. Dissociative and non-dissociative free electron capture cross-sections of C_2Cl_4 (left) and C_2HCl_3 (right).

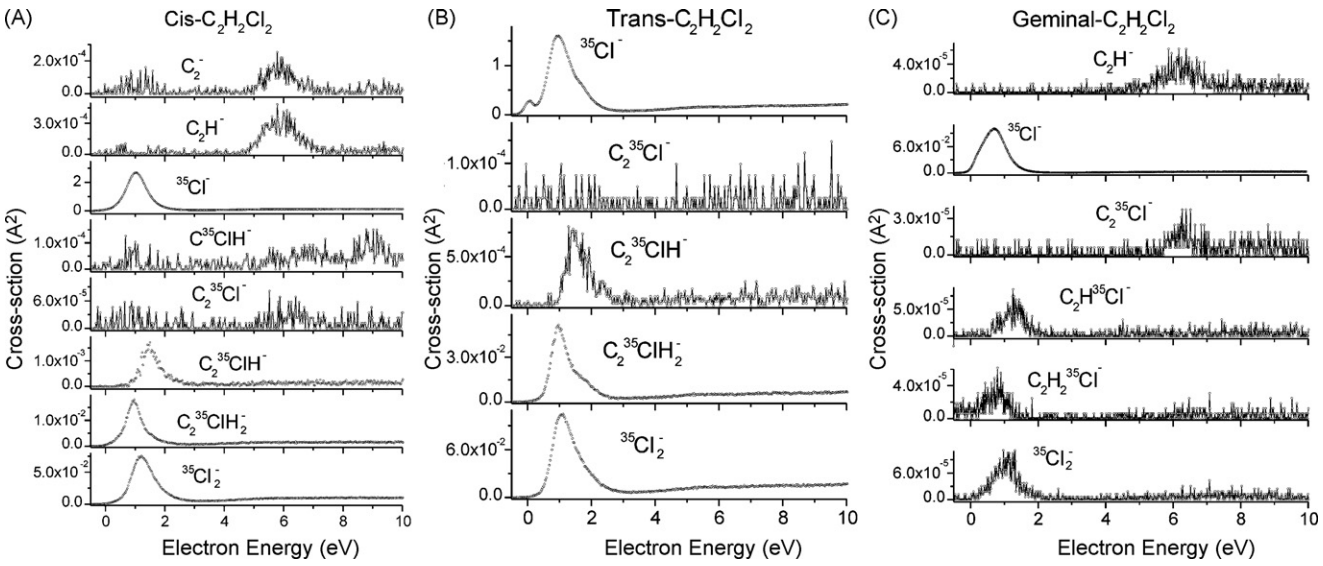

Fig. 2. Dissociative free electron capture cross-sections of *cis*- (A), *trans*- (B), and geminal-$C_2H_2Cl_2$ (C).

4. Results and discussion

4.1. Chloro-ethylenes

All of the chloro-ethylenes studied showed formation of Cl^- as the main fragmentation process under REC conditions (Figs. 1 and 2). Other fragment NIs were found to have much lower cross-sections and peaked at higher energies than that for the Cl^-. The resonance electron attachment cross-section for perchloro-ethylene, C_2Cl_4 (Fig. 1), for example, showed very efficient dissociative and moderate non-dissociative electron capture at low-energies in full accord with previous reports on the compound [4,9,16,17], where only relative electron capture cross-sections were determined similar to the present crossed-beam experiments.

For the two compounds, C_2Cl_4 and C_2HCl_3, long-lived molecular NIs were detected at electron energies near 0 eV. Molecular NIs for C_2Cl_4 have been reported previously [4,9,11,12,15,16], but the long-lived $C_2HCl_3^-$ species, as far as we know, is observed here for the first time. Due to relatively pure energy resolving power of the present experiments (ca. 60 meV), observed non-dissociative electron attachment cross-sections for both $C_2Cl_4^-$ and $C_2HCl_3^-$ (Fig. 1) at energies near to 0 eV is the result of convolution of real cross-section with the instrumental function and therefore numbers presented in Fig. 1 for the case of $C_2Cl_4^-$ and $C_2HCl_3^-$ at energies near to 0 eV are rather meaningful. On the other hand, observation of these species is a strong indication that these molecular NIs are long-lived and that their lifetimes are within experimental time-frame for detection with our instrument.

The formation cross-section of Cl^- from $C_2Cl_4^-$ and $C_2HCl_3^-$ at energies lower than ca. 50 meV is also distorted by limited energy resolving power (Figs. 3 and 4) of the instrument. However, higher energy values are reliable within the accuracy of our measurements. These NIs have been recorded at two temperatures of the molecular beam. Whereas little difference was observed in the case of C_2Cl_4 at the two temperatures, a more pronounced effect was apparent in the case of C_2HCl_3. These findings are remarkable and need special analysis. To understand why C_2HCl_3 molecular NIs were not observed in the earlier experiments we resorted to statistical Rice–Ramsperger–Kassel–Marcus theory to estimate the rate constants (reciprocal of mean lifetimes) with respect to electron autodetachment for both molecular NIs of $C_2Cl_4^-$ and $C_2HCl_3^-$ (Fig. 5 and Fig. S1, [39]). For this we used a similar approach that was developed earlier [40,41] for the fullerene NIs. The theoretical rate constant for electron autodetachment of $C_2Cl_4^-$ (Fig. 5) fits within the limits of earlier experimentally determined [15] lifetimes, i.e., 3–130 μs. A very steep rise in the theoretical rate constant curve at low electron energies near 0 eV that is accessible in Rydberg electron transfer (RET) spectroscopy [15] explains nicely the broad range of experimentally observed lifetimes. Similarly [41], we also averaged the rate constants over the whole ensemble using canonical distribution and another distribution derived by Andersen et al. [42] (see Fig. S2). The results from averaging to even higher net rate constants at low internal energies pushing them out of the

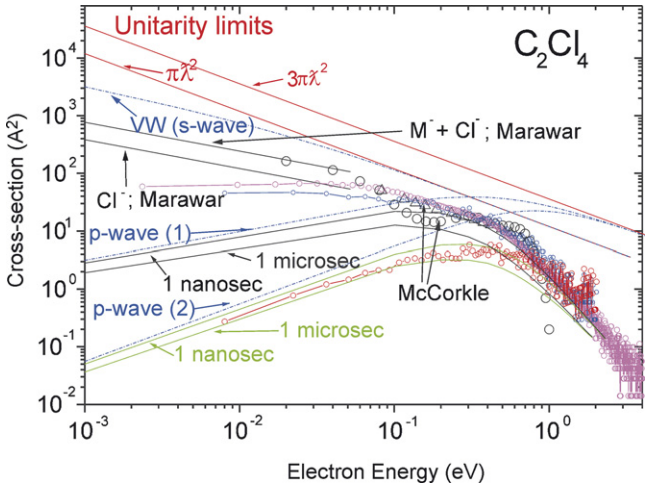

Fig. 3. Cross-sections for the formation of Cl^- from C_2Cl_4 at two molecular temperatures (40 °C – small blue circles); 120 °C – small magenta circles; from C_2Cl_4; Cl^- cross-section at 40 °C divided by E^{-1} (E is electron energy) to compensate for the contribution from s-wave capture; theoretical limits for the s-wave and p-wave electron capture (red solid lines); Vogt–Wannier (VW) cross-section for the s-wave capture (blue dash-dot line); p-wave capture cross-sections calculated for two models, 1 and 2 (blue dash-dot lines; see text); cross-sections modified by inclusion of electron autodetachment after 1 ns and 1 μs for model 1 (black lines) and model 2 (green lines); experimental cross-sections for M^- and Cl^- together and Cl^- separately taken from Marawar et al. [12] (black lines); electron attachment cross-sections from swarm data by McCorkle et al. [10] obtained with an unfolding procedure (large black circles) and Eq. (2) (black up-triangles).

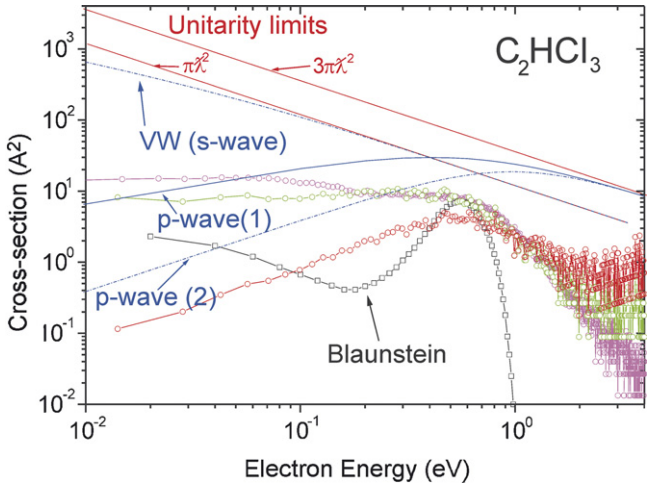

Fig. 4. Cross-section formation of Cl^- from C_2HCl_3 at two molecular temperatures (40 °C – green circles); 120 °C – magenta circles; from C_2HCl_3; Cl^- cross-section at 40 °C divided by E^{-1} (E is electron energy) to compensate for the contribution from s-wave capture (red circles); theoretical limits for the s-wave and p-wave electron capture (red solid lines); Vogt–Wannier (VW) cross-section for s-wave capture (blue dash-dot line); p-wave capture cross-sections calculated via two models 1 (blue solid line) and 2 (blue dash-dot line; see text); electron attachment cross-sections from swarm data by Blaunstein and Christophorou [6] obtained with an unfolding procedure (black squares).

measurable lifetime range typical of the mass spectrometry time domain. At higher internal energies the discrepancy between the delta-function and more realistic canonical or Andersen's et al. [42] distributions gets very small. It is beyond the main purpose of this paper to consider these questions, but it is clear that depletion at low mean energies that result in the fast loss of the most excited species of the ensemble should be taken into account. In the case of fullerenes [41], this process was estimated and was included in the net results after comparison of the theoretical and experimental rate constants over a broad energy range. Here we do not have this opportunity and special work would have to be done to include this physical process in the final estimation of the rate constant. Similar estimates of the $C_2HCl_3^-$ lifetime (Fig. S1) predicted higher rate constants near the threshold energy in comparison to that of $C_2Cl_4^-$. It is remarkable that the autodetachment rate constant for $C_2HCl_3^-$ just "touches" the upper limit of the typical mass spectrometer time domain. Our compact instrument with its very short total ion-flight distance [33,34], made it possible to observe these species of $C_2HCl_3^-$; earlier investigations of this kind [4,9] failed, perhaps because of the much longer flight times (~40 μs [4]) in comparison to ours (<10 μs) (one should note that long-lived species of $C_2Cl_4^-$ and $C_2HCl_3^-$ observed by the Chen et al. [28] were obtained under chemical ionization conditions, i.e., well beyond single-collision events, and therefore these results cannot be compared directly with the present or similar beam measurements). To some extent, this finding for $C_2HCl_3^-$ is similar to earlier observations on *para*-aminoazobenzene wherein long-lived molecular NIs survived to be recorded only as neutral species from corresponding NIs that underwent electron autodetachment in the second field-free region of the mass spectrometer [43].

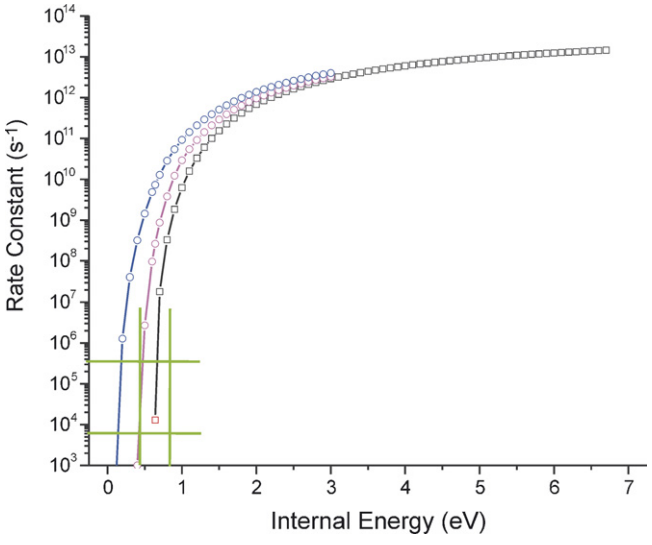

Fig. 5. Rate constants for electron autodetachment from $C_2Cl_4^-$ with electron affinity 0.64 eV [28] (black squares; the first calculated point that is within the experimental time frame (μs) marked in red) with energy distribution as delta-function; same for Andersen distribution [42] (magenta circles) and canonical distribution (blue circles); green horizontal lines indicate range of experimentally [15] measured lifetimes and green vertical lines indicate Andersen distribution FWHM of $C_2Cl_4^-$ at internal energy of 0.64 eV (i.e., 0 eV electron attachment; see text).

Based on this statistical model for $C_2Cl_4^-$, survival ion fractions for typical energy ranges of RET spectroscopy, have been calculated using Andersen's [42] distribution (Fig. S3); these can be compared with the corresponding experimental results [15]. Theoretical predictions (Fig. S3) match the experimentally determined ion fractions [15] rather well as both show that approximately half the amount of initially formed NIs should survive within tens of μs at low electron energies.

The Illenberger and Märk groups [16] discovered four NI states in the case of $C_2Cl_4^-$ over an energy range of 0.4–1.4 eV by dividing Cl^- yield by E^{-1} thus compensating for the contribution of s-wave electron attachment. The resonance peaks obtained in such a manner become especially prominent by increasing the sample pressure just a little. Having comparable energy resolution and using the same procedure, we did not observe similar structures in the Cl^- cross-section curve for the same energy range (Fig. 3, red circles). To understand the energy behavior in the cross-section curves, we used Vogt–Wannier (VW) [44] and Levy-Keller (LK) [45] theories that dealt with electron scattering and capture by a long-range ($-\alpha/r^\nu$; $3 < \nu < 5$; α is the molecular polarizability [46]) potential. We believe that at low energies, the cross-section in the case of C_2Cl_4 should follow the VW predictions for the s-wave. However the limited energy resolving power of our instrument prevented us from proving it. Nevertheless, the much better resolution used in the RET experiments [12] showed similarities with the VW theory-derived behavior at low energies although the experimentally determined absolute cross-sections were lower than theoretical predictions. p-Wave cross-sections derived from the LK-theory with $\nu = 4$ (model 2; blue dash-dot line in Fig. 3) match the modified experimental cross-sections at low-energies (Fig. 3; red circles) very well. Although this theoretical cross-section curve reaches the p-wave unitarity limit at higher energies, it does not follow the Wigner threshold behavior ($\propto E^{l-1/2}$) [47] at low energies and the good matches with the modified experimentally determined curve, just could be fortuitous. Since the modified experimental cross-section also does not follow the Wigner threshold law, either modification procedure of the experimental cross-section is not entirely valid, or higher than p-wave harmonics also can contribute to the Cl^- formation cross-section in the energy range being considered. Modified LK-theory with ν slightly lower than 4 (model 1; another blue dash-dot line in Fig. 3) nicely follows both the unitarity limit at high energies and the Wigner behavior at lower energies. However, experimental cross-sections, both modified and non-modified, show a rather strong decrease with energy in comparison to theoretical cross-sections. Such dramatic differences in experimental and theoretical cross-sections can be associated

with electron autodetachment processes that are in permanent and strong competition with fragmentation of NIs. Indeed, after inclusion of electron autodetachment calculated on the basis of RRKM theory, the match between theory and experiment gets much better, especially for ions that survive as long as nanoseconds before dissociating (Fig. 3). This means that the main contribution in Cl^- formation cross-section within the energy range ~100 meV to several eV is due to molecular NIs that the fragment over a period of several nanoseconds. Of course, slower fragmentation processes (up to 1–2 μs, i.e., till the time when NIs leave the ion source) also result in Cl^- formation but their contributions are much lower. What is also important is that fast electron autodetachments have little influence on the Cl^- formation processes. That means that initially formed shape resonances contribute to the survival of NIs until pure statistical processes in ion evolution become dominant. This finding is proof of fragmentation occurring via predissociation processes when initially formed π^* shape resonances evolves into different repulsive states associated with σ^* (C—Cl) resonances. Clearly, only such slow fragmentation can explain the rather low translational energy release observed for Cl^- from C_2Cl_4 [13]. The issue concerning different fragmentation mechanisms for $C_2Cl_4^-$ that result in Cl^- formation, have been thoroughly discussed in the literature [4,9,13,16,17,26,27]. Our calculations on electron autodetachment processes have been carried out for a model of $C_2Cl_4^-$ and a transition state where excitation of the C=C stretching mode played a central role. The model therefore presumed not only involvement of a π^* (C=C) shape resonance as the initial ion formation process, but more dramatically that the NI ground state should be molecule plus an extra electron on the π^* orbital. Other models of $C_2Cl_4^-$ with a σ^* (C—Cl) resonance as ground state, as has been suggested [26], were not considered; we hope to return to this question in the future.

Other chloro-ethylenes under study also showed Cl^- formation as dominant decay processes of the molecular NIs (Figs. 1, 2 and 4, Figs. S4–S6). It is interesting that three dichloro-isomers of ethylenes showed distinct absolute NI formation cross-sections with the *cis*-isomer having the highest Cl^- formation cross-section and the geminal isomer possessing the lowest one. Adiabatic electron affinities of these isomers are supposed to be either very low or even negative. That is why the deviation of experimental and theoretical (without including electron autodetachment) cross-sections is so dramatic (Figs. S4–S6) when compared to those for C_2Cl_4 and C_2HCl_3. It is interesting that the energy of the Cl^- maximum yield for these isomers quite nicely follows the energies for π^* shape resonances as determined by electron transmission spectroscopy (ETS) and by quantum chemical calculations (QCC). Computations were performed by 6-31G(d) level of theory using scaling procedures [35,36]). Thus the comparative results were: C_2Cl_4: <0.12 eV (ETS: 0.3 eV [18]; 0.4 eV [17]; QCC: 0.358 eV); C_2HCl_3: 0.5 eV (ETS: 0.59 eV [18]; 0.61 eV [17]; QCC: 0.574 eV); *cis*-$C_2H_2Cl_2$: 1.0 eV (ETS: 1.11 eV [18]; 1.12 eV [17]; QCC: 0.99 eV); *trans*-$C_2H_2Cl_2$: 0.91 eV (ETS: 0.8 [18]; 0.83 [17]; QCC: 0.899 eV); geminal-$C_2H_2Cl_2$: 0.69 eV (0.76 eV [18]; 0.75 eV [17]; QCC: 0.95 eV). The same trend was observed earlier by others [4,17]; the only exception being from the Illenberger laboratory [4] wherein the Cl^- peak from *trans*-$C_2H_2Cl_2$ appeared at higher energy than was observed in ETS studies. Bearing in mind the above correlations, it is especially interesting that geminal-C_2HCl_2 which is observed with the lowest resonance energy, nevertheless, has the lowest Cl^- formation cross-section amongst all three isomers. It is assumed that competition between fragmentation and electron autodetachment is much stronger for this compound than it is for the other two isomers. This in itself may be a consequence of the lower adiabatic electron affinities of the latter compounds. This conclusion, however, is at variance with earlier studies [26] using the so-called "negative ion chemical ionization" approach in which it was reported that the electron affinities were 0.1 eV for all isomers. Clearly, the present data do not support that finding.

Johnson et al. [9] addressed the question of Cl_2^- formation from the dichloro-ethylenes isomers. It was concluded that the relative production of these NIs is stronger when Cl atoms are located on the adjacent carbon atoms. Indeed, not only the relative but also the absolute Cl_2^- formation cross-section is very low in the case of geminal-$C_2H_2Cl_2$ (Fig. 2). The results were explained [9] on the basis of the formation of a structure with two unpaired electrons on the same carbon atom, which is energetically very unfavorable. If one considers the results for the *cis*- and *trans*-$C_2H_2Cl_2$ isomers, it is clear (Fig. 2) that Cl_2^- formation cross-sections for these two isomers are similar, being somewhat larger in the case of the *trans*-isomer. This fact is a bit surprising if one takes into account the spatial separation between the two chorine atoms, which is greater for the *trans*-isomer. Further theoretical analysis is required to understand this observation.

Except for *trans*-$C_2H_2Cl_2$, other chloro-ethylenes showed NI formation processes at energies just below the characteristic singlet–singlet transitions in neutral molecules [24,25] (Figs. 1 and 2). Perhaps, electronically excited Feshbach resonances are the parent states for these fragment ions. In all compounds, however, the absolute dissociative electron attachment cross-sections for these resonances are much lower than those for similar processes at lower energies, where presumably shape resonances are involved.

The results reported in the literature, i.e., mainly from swarm experiments for determining electron attachment rate constants by the Christophorou group [6–10], showed quite reasonable agreement with those presented here (Figs. 3 and 4, Figs. S4–S6). It is interesting that the shapes of the cross-section curves versus the electron energy match up very well with the cross-section values that were calculated with a simple equation (2) using data from the literature [10,48]:

$$\sigma_{\{\varepsilon\}} = \frac{k(T)}{\langle v \rangle}, \tag{2}$$

where $\sigma_{\{\varepsilon\}}$ is the value of the cross-section at electron energy $\{\varepsilon\} = k_B T_e$, $\langle v \rangle$ is the mean thermal velocity of electrons at electron temperature T_e and $k(T)$ the electron attachment rate constant determined at molecular temperature T. We refer the reader to Ref. [48] where validity of this simple approach is discussed. In some cases, electron attachment cross-sections reported in the literature have been obtained by an unfolding procedure of swarm data. These absolute electron attachment cross-sections match the present results rather well for those taken at the maximum yield. But the shapes of the cross-sections as a function of energy are rather different, as they very often show a rather abrupt decrease in the unfolded cross-sections at higher energies. We believe that such behavior is associated with an artifact of the unfolding procedure and that the present beam cross-sections are more realistic in this energy range. Moreover, the unfolded data appear to experience an additional energy shift of ~0.2 eV (see discussions [17]). Before comparing the swarm results with the present data (Figs. 3 and 4, Figs. S4–S6), a correction of the energy scale was made for the former. Marawar et al. [12] in comparing their RET data with those from swarm experiments [10] noted that the cross-sections determined by the unfolding swarm measurements were somewhat larger. They rationalized this discrepancy on the basis of collisional stabilization of the molecular NIs with buffer gas molecules in the swarm experiments. Our data were also obtained under single collision conditions similar to those in the RET experiments. However, the agreement of the present data with those from the swarm experiments is better. We extrapolated the RET results up to 40 meV, using equations for determining cross-sections [10] in

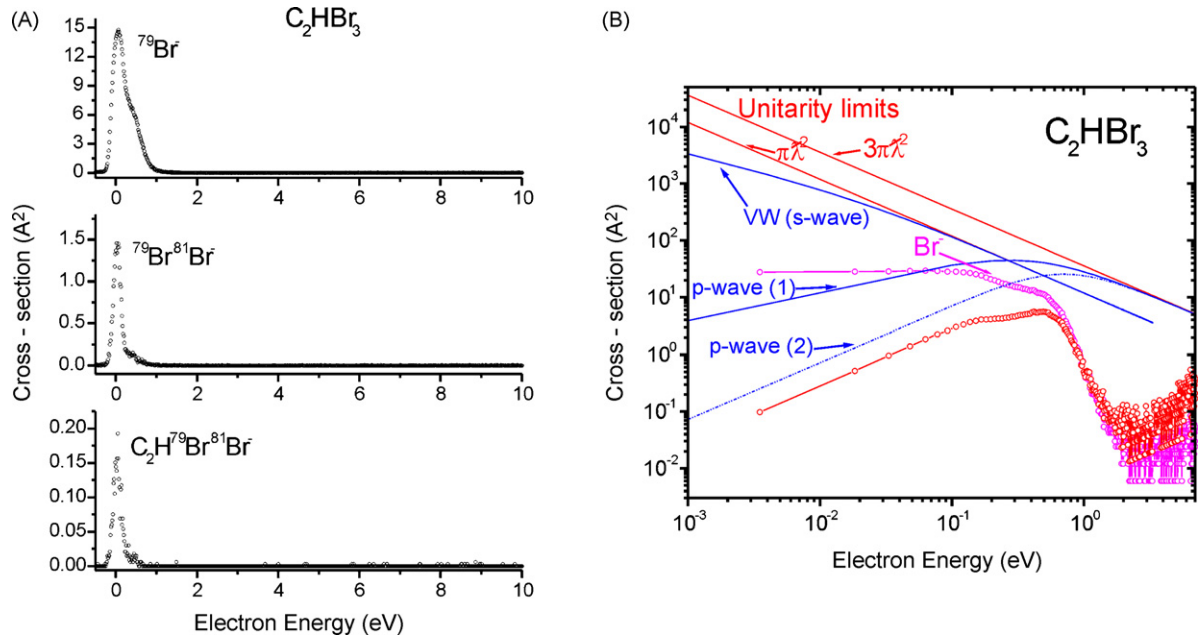

Fig. 6. (A) Dissociative free electron capture cross-sections for negative ions from C_2HBr_3 and (B) cross-section formation of Br^- from C_2HBr_3 (magenta circles); Br^- cross-section divided by E^{-1} (E is electron energy) to compensate for the contribution from s-wave capture (red circles); theoretical limits for s-wave and p-wave electron capture (red solid lines); Vogt–Wannier (VW) cross-section for s-wave capture (blue dash-dot line); p-wave capture cross-sections calculated via models 1 (blue solid line) and 2 (blue dash-dot line; see text).

order to make realistic comparisons with our results. We are not aware whether the reported signals for M^- and Cl^- in the RET measurements [10] included contributions from the ^{37}Cl isotope, but if one assumes that only the ^{35}Cl isotope was considered, then after including the contribution from ^{37}Cl, we find the RET results to be in much better agreement with those from both the present and the swarm experiments (Fig. 3). It is to be noted that all Cl^- formation cross-sections (Figs. 3 and 4, Figs. S4–S6) include contributions from both chlorine isotopes, whereas those shown in Figs. 1 and 2 depict cross-sections only for the indicated isotope.

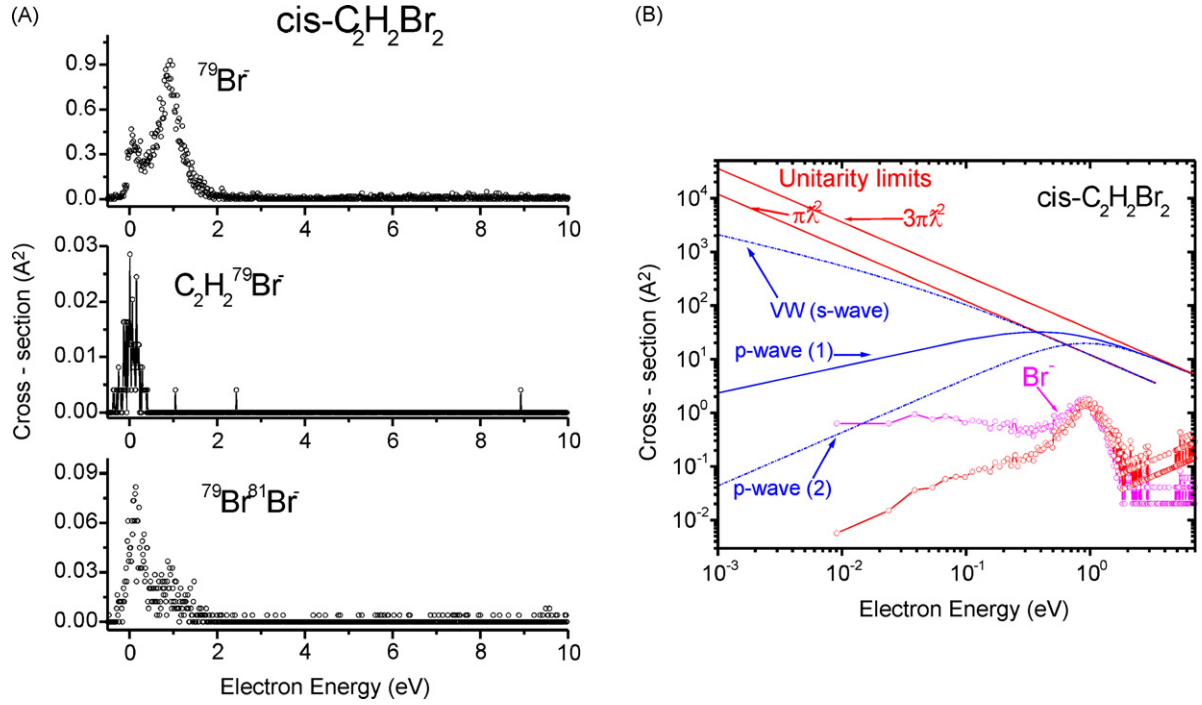

Fig. 7. (A) Dissociative free electron capture cross-sections for negative ions from *cis*-$C_2H_2Br_2$; (B) cross-section formation of Br^- from *cis*-$C_2H_2Br_2$ (magenta circles); Br^- cross-section divided by E^{-1} (E is electron energy) to compensate for the contribution from s-wave capture (red circles); theoretical limits for s-wave and p-wave electron capture (red solid lines); Vogt–Wannier (VW) cross-section for s-wave capture (blue dash-dot line); p-wave capture cross-sections calculated via models 1 (blue solid line) and 2 (blue dash-dot line; see text).

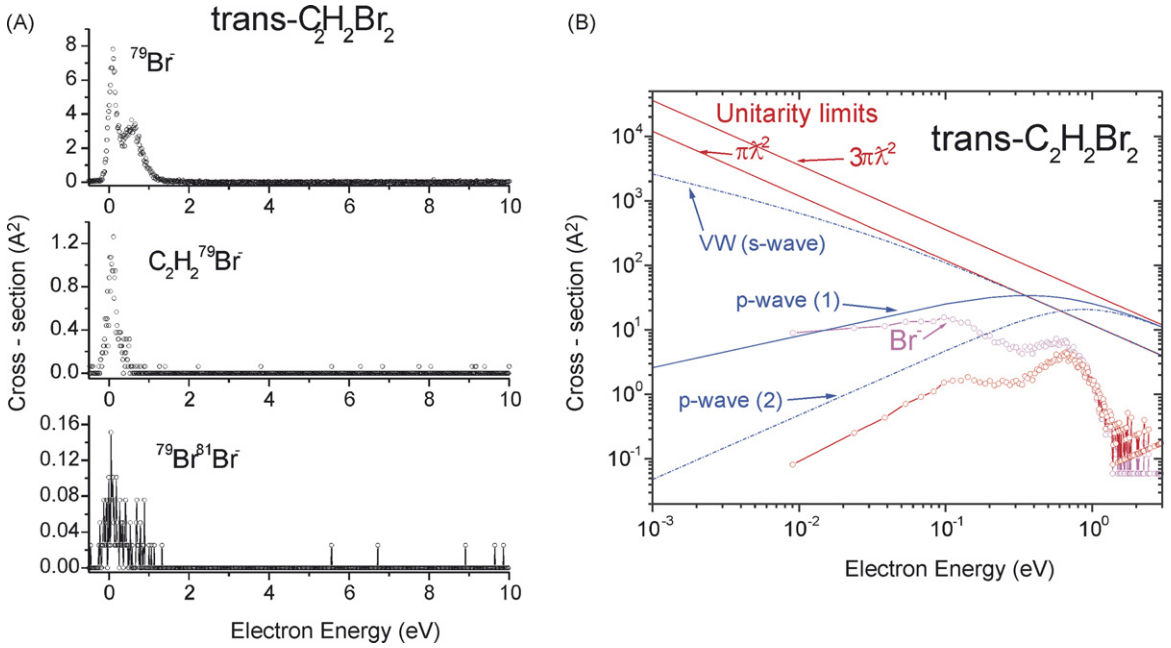

Fig. 8. (A) Dissociative free electron capture cross-sections for negative ions from *trans*-$C_2H_2Br_2$; (B) cross-section formation of Br^- from *trans*-$C_2H_2Br_2$ (magenta circles); Br^- cross-section divided by E^{-1} (E is electron energy) to compensate for the contribution from s-wave capture (red circles); theoretical limits for s-wave and p-wave electron capture (red solid lines); Vogt–Wannier (VW) cross-section for s-wave capture (blue dash-dot line); p-wave capture cross-sections calculated via models 1 (blue solid line) and 2 (blue dash-dot line; see text).

4.2. Bromo-ethylenes

As far as we are aware, absolute negative ion electron attachment cross-sections for bromo-ethylenes have not been reported in the literature. The present data (Figs. 6–9) are the first of its kind. These measurements were carried out under conditions similar to those for the chloro-ethylenes. It was suggested in the present experiments that the detection efficiencies of the Br^- and Cl^- (from the calibrant compounds) at the multi-channel plate detector of our instrument were very close at the 2 keV impact energy. In contrast to chloro-ethylenes, no long-lived parent NIs were observed for the bromo-ethylenes studied. In general, dissociative electron attachment cross-sections of bromo-ethylenes were found to be larger than that of chloro-ethylenes and the resonance maxima of Br^- yields occur at lower energies than those of Cl^- from chlorethylenes. These results are similar to those reported

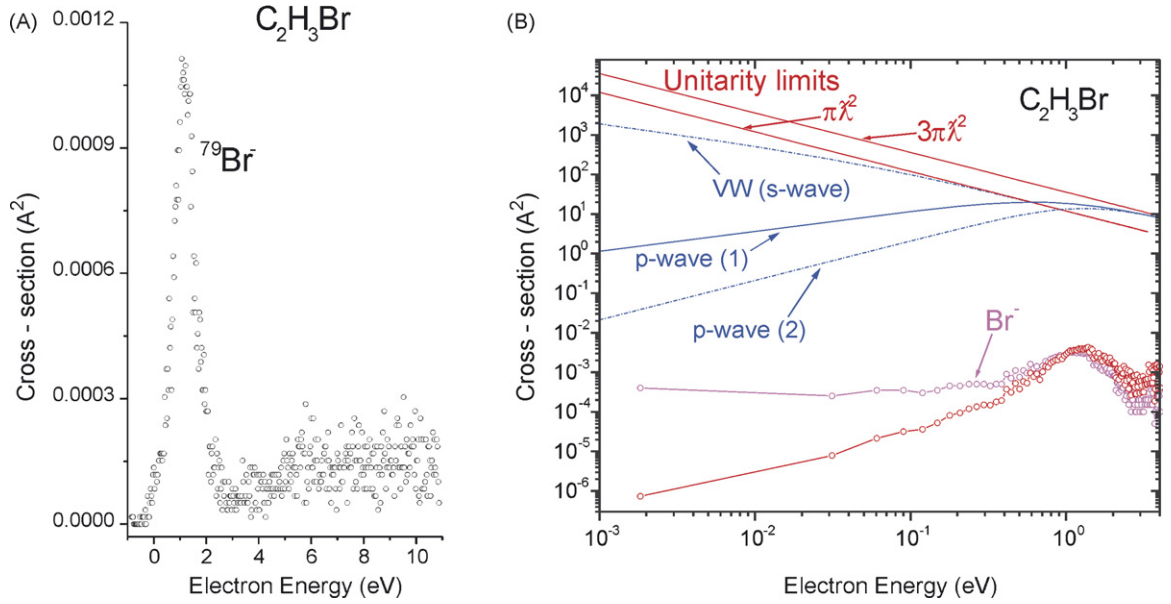

Fig. 9. (A) Dissociative free electron capture cross-section for $^{79}Br^-$ formation from C_2H_3Br; (B) cross-section formation of Br^- from C_2H_3Br (magenta circles); Br^- cross-section divided by E^{-1} (E is electron energy) to compensate for the contribution from s-wave capture (red circles; the line connecting circles serves to guide the eye); theoretical limits for s-wave and p-wave electron capture (red solid lines); Vogt–Wannier (VW) cross-section for s-wave capture (blue dash-dot line); p-wave capture cross-sections calculated via models 1 (blue solid line) and 2 (blue dash-dot line; see text).

by Underwood-Lemons et al. [23] for larger chloro- and bromo-alkenes. In contrast to chloro-ethylenes, where formation of Cl^- apparently is the predominant fragmentation pathway, bromo-ethylenes showed much less differentiation in electron attachment cross-sections amongst various fragmentation channels, although here again the cross-section for Br^- production is the highest (Figs. 6–9). Unfortunately, the limited energy resolving power in the present experiments does not allow precise determination of cross-sections at very low electron energies, but again at higher energies, cross-sections are not affected by the energy resolving power. As in the case of chlorinated compounds, the difference between the theoretical cross-section for p-wave electron attachment and experimental data is supposedly affected by electron autodetachment.

To our knowledge, the only relevant ETS spectrum reported so far has been that of C_2H_3Br [22]. Thus, except for this compound, the correlation of Br^- maximum yield and energies of shape resonances can be done only by a comparison with calculated values obtained by 6-31G(d) level of theory with a scaling procedure [35,36]: C_2HBr_3: ca. 0 and 0.5 eV (QCC: 0.35 eV (σ^*) and 0.521 eV (π^*)); *cis*-$C_2H_2Br_2$: 0.92 eV (QCC: 0.87 eV); *trans*-$C_2H_2Br_2$: 0.61 eV QCC: 0.8 eV); C_2H_3Br: 1.11 eV (1.17 eV [22]; QCC: 1.24 eV).

Another interesting distinction observed here is that the cross-section for Br^- production from *trans*-$C_2H_2Br_2$ is higher than that of the *cis*-isomer (Figs. 14 and 15). These compounds were bought from Sigma–Aldrich as a mixture, but were separated by gas-chromotography before their introduction into the mass spectrometer. Preliminary results on the separation and detection by REC mass spectrometry was reported earlier [34]. NMR analysis of the mixture showed that the *trans*- and *cis*-isomers were present in a 1:3 molar ratio. Dissociative electron attachment spectra of the mixture introduced via a liquid port without separation of its components is presented (Fig. S7) and only a comparison with spectra of separated compounds helps make assignment of the resonance peaks.

In the case of monobromo-ethylene, we were able to observe the only fragment Br^- NI (Fig. 9). Its production has been found to occur with a rather small cross-section, perhaps even smaller than that of its chlorinated counterpart, C_2H_3Cl [10]. This observation needs further theoretical investigation.

5. Conclusions

The absolute dissociative electron capture cross-sections for molecules of chloro- and bromo-ethylenes have been studied using a recently designed and constructed GC–REC-rTOF-MS. It was proved that interface of the GC and REC-MS can provide a unique opportunity for measuring absolute dissociative and non-dissociative electron attachment cross-sections with relatively high accuracy and precision. Tetra and tri-chlorinated ethylenes have been found to form long-lived (i.e., mass spectrometrically detectable) molecular NIs, M^-. Herein is reported the first observation of the molecular NI for C_2HCl_3. The measurements of absolute cross-sections for non-dissociative electron capture forming M^- and one of the dissociative channels that result in the generation of Cl^- NIs, indicated a strong bias for the fragmentation process. Although all NIs are known to be formed from intermediate resonance states of M^-, fragmentation into smaller species is not the only decay process for M^-. Electron autodetachment significantly lowers the observable absolute non-dissociative electron capture cross-sections. Tetra-brominated ethylene was not studied here but the tri-, di- and mono-brominated ethylenes were found not to form long-lived M^-. Interesting differences in low-energy absolute dissociative electron capture cross-sections between isomers of di-halogenated ethylenes for both Cl and Br have been revealed. These differences are in line with theoretical predictions made on the basis of potential scattering theory modified by inclusion of the ion depletion effect due to electron autodetachment.

Acknowledgements

This project was supported by individual NIH research grants ES09536 and ES10338, by the NIEHS grant ES00210 and by the W.M. Keck foundation award. This publication was made possible in part by grant number P30 ES00210 from the National Institute of Environmental Health Sciences, NIH. The authors wish to acknowledge the Mass Spectrometry Facility of the Environmental Health Sciences Center at Oregon State University. We would like to express our gratitude to Prof. Victor Hsu for assistance in the NMR analysis of the *cis–trans* mixture of dibromo-ethylene.

Appendix A. Supplementary data

Supplementary data associated with this article can be found, in the online version, at doi:10.1016/j.ijms.2008.07.008.

References

[1] T. Oster, A. Kühn, E. Illenberger, Int. J. Mass Spectrom. Ion Processes 89 (1989) 1 (review with references therein).
[2] O. Ingólfsson, F. Weik, E. Illenberger, Int. J. Mass Spectrom. Ion Processes 155 (1996) 1 (review with references therein).
[3] E. Illenberger, Chem. Rev. 92 (1992) 1589 (review with references therein).
[4] R. Kaufel, E. Illenberger, H. Baumgärtel, Chem. Phys. Lett. 106 (1984) 342.
[5] E. Illenberger, H. Baumgärtel, S. Süzer, J. Electron Spectrosc. Relat. Phenom. 33 (1984) 123.
[6] R.P. Blaunstein, L.G. Christophorou, J. Chem. Phys. 49 (1968) 1526.
[7] A.A. Christodoulides, L.G. Christophorou, J. Chem. Phys. 54 (1971) 4691.
[8] L.G. Christophorou, Chem. Rev. 76 (1976) 409.
[9] J.P. Johnson, L.G. Christophorou, J.G. Carter, J. Chem. Phys. 67 (1977) 2196.
[10] D.L. McCorkle, A.A. Christodoulides, L.G. Christophorou, in: L.G. Christophorou, M.O. Pace (Eds.), Gaseous Dielectrics IV, vol. 4, Pergamon, New York, NY, 1984, pp. 12.
[11] S.H. Alajajian, A. Chutjuan, J. Phys. B: Atom. Mol. Opt. Phys. 20 (1987) 2117.
[12] R.W. Marawar, C.W. Walter, K.A. Smith, F.B. Dunning, J. Chem. Phys. 88 (1988) 176.
[13] C.W. Walter, K.A. Smith, F.B. Dunning, J. Chem. Phys. 90 (1989) 1652.
[14] R.A. Popple, M.A. Dionne, K.A. Smith, F.B. Dunning, J. Chem. Phys. 107 (1994) 5672.
[15] L. Suess, R. Parthasarathy, F.B. Dunning, J. Chem. Phys. 118 (2003) 6205.
[16] H. Drexel, W. Sailer, V. Grill, P. Scheier, E. Illenberger, T.D. Märk, J. Chem. Phys. 118 (2003) 7394.
[17] J.K. Olthoff, J.A. Tossel, J.H. Moore, J. Chem. Phys. 83 (1985) 5627.
[18] P.D. Burrow, A. Modelli, N.S. Chiu, K.D. Jordan, Chem. Phys. Lett. 82 (1981) 270.
[19] K.L. Stricklett, S.C. Chu, P.D. Burrow, Chem. Phys. Lett. 131 (1986) 279.
[20] Y. Choi, K.D. Jordan, Chem. Phys. Lett. 156 (1989) 450.
[21] A. Modelli, Phys. Chem. Chem. Phys. 5 (2003) 2923.
[22] A. Modelli, D. Jones, J. Phys. Chem. A 108 (2004) 417.
[23] T. Underwood-Lemons, G. Saghi-Szabo, J.A. Tossell, J. Chem. Phys. 105 (1996) 7896.
[24] J.H. Moore Jr., J. Phys. Chem. 76 (1972) 1130.
[25] C.F. Koerting, K.N. Walzi, A. Kuppermann, Chem. Phys. Lett. 109 (1984) 140.
[26] E. Desai D'sa, W.E. Wentworth, E.C.M. Chen, J. Phys. Chem. 92 (1988) 285.
[27] J.R. Willey, E.C.M. Chen, W.E. Wentworth, J. Phys. Chem. 97 (1993) 1256.
[28] E.C.M. Chen, J.R. Willey, C.F. Batten, W.E. Wentworth, J. Phys. Chem. 98 (1994) 88.
[29] P.J. Squillace, M.J. Moran, W.W. Lapham, C.V. Price, R.M. Clawges, J.S. Zogorski, Environ. Sci. Technol. 33 (1999) 4176.
[30] R.E. Doherty, J. Environ. Forensics 1 (2000) 69.
[31] C.J. Gantzer, L.P. Wackett, Environ. Sci. Technol. 25 (1991) 715.
[32] C. Holliger, G. Wohlfarth, G. Diekert, FEMS Microbiol. Rev. 22 (1999) 383.
[33] V.G. Voinov, Y.V. Vasil'ev, J. Morré, D.F. Barofsky, M.L. Deinzer, M. Gonin, T.F. Egan, K. Führer, Anal. Chem. 75 (2003) 3001.
[34] V.G. Voinov, Y.V. Vasil'ev, H. Ji, B. Figard, J. Morré, T.F. Egan, D.F. Barofsky, M.L. Deinzer, Anal. Chem. 76 (2004) 2951.
[35] K. Aflatooni, B. Hitt, G.A. Gallup, P.D. Burrow, J. Chem. Phys. 115 (2001) 6489.
[36] K. Aflatooni, G.A. Gallup, P.D. Burrow, J. Phys. Chem. A 104 (2000) 7359.
[37] S.C. Chu, P.D. Burrow, Chem. Phys. Lett. 172 (1990) 17.
[38] K. Aflatooni, P.D. Burrow, J. Chem. Phys. 113 (2000) 1455.
[39] All figures mentioned in the text that are in the Supplementary Data have letter S with the running numbers.

[40] Y. Vasil'ev, R. Absalimov, S. Nasibullaev, A. Lobach, T. Drewello, J. Phys. Chem. A 105 (2001) 661.
[41] Y.V. Vasil'ev, R.R. Abzalimov, S.K. Nasibullaev, T. Drewello, Fullerene Nanotubes Carbon Nanostruct. 12 (2004) 229.
[42] J.U. Andersen, E. Bonderup, K. Hansen, J. Chem. Phys. 114 (2001) 6518.
[43] Y.V. Vasil'ev, V.A. Mazunov, Doklady AN SSSR 315 (1990) 637 (in Russian) (Sov. Chem. Phys. Doklady (in English)).
[44] E. Vogt, G.H. Wannier, Phys. Rev. 95 (1954) 1190.
[45] B.R. Levy, J.B. Keller, J. Math. Phys. 4 (1963) 54.
[46] T.M. Miller, in: D.R. Lide (Ed.), CRC Handbook of Chemistry and Physics, CRC Press, Taylor and Francis, Boca Raton, 2005–2006, pp. 10, 192–201.
[47] E.P. Wigner, Phys. Rev. 73 (1948) 1002.
[48] J.D. Skalny, S. Matejcik, T. Mikoviny, J. Vencko, G. Senn, A. Stamatovic, T.D. Märk, Int. J. Mass Spectrom. 205 (2001) 77.